DRILLING THROUGH GAS HYDRATES FORMATIONS: MANAGING

WELLBORE STABILITY RISKS

A Thesis

by

TAGIR R. KHABIBULLIN

Submitted to the Office of Graduate Studies of
Texas A&M University
in partial fulfillment of the requirements for the degree of

MASTER OF SCIENCE

August 2010

Major Subject: Petroleum Engineering

Drilling Through Gas Hydrates Formations: Managing Wellbore Stability Risks

DRILLING THROUGH GAS HYDRATES FORMATIONS: MANAGING

WELLBORE STABILITY RISKS

A Thesis

by

TAGIR R. KHABIBULLIN

Submitted to the Office of Graduate Studies of
Texas A&M University
in partial fulfillment of the requirements for the degree of

MASTER OF SCIENCE

Approved by:

Co-Chairs of Committee,	Gioia Falcone
	Catalin Teodoriu
Committee Member,	Mitch Lyle
Head of Department,	Steve Holdich

August 2010

Major Subject: Petroleum Engineering

ABSTRACT

Drilling Through Gas Hydrates Formations: Managing Wellbore Stability Risks.

(August 2010)

Tagir R. Khabibullin, B.S., Ufa State Petroleum Technological University, Ufa

Co-Chairs of Advisory Committee: Dr. Gioia Falcone
                                       Dr. Catalin Teodoriu

As hydrocarbon exploration and development moves into deeper water and onshore arctic environments, it becomes increasingly important to quantify the drilling hazards posed by gas hydrates.

To address these concerns, a 1D semi-analytical model for heat and fluid transport in the reservoir was coupled with a numerical model for temperature distribution along the wellbore. This combination allowed the estimation of the dimensions of the hydrate-bearing layer where the initial pressure and temperature can dynamically change while drilling. These dimensions were then used to build a numerical reservoir model for the simulation of the dissociation of gas hydrate in the layer. The bottomhole pressure (BHP) and formation properties used in this workflow were based on a real field case.

The results provide an understanding of the effects of drilling through hydrate-bearing sediments and of the impact of drilling fluid temperature and BHP on changes in temperature and pore pressure within the surrounding sediments. It was found that the amount of gas hydrate that can dissociate will depend significantly on both initial formation characteristics and bottomhole conditions, namely mud temperature and

pressure. The procedure outlined suggested in this work can provide quantitative results of the impact of hydrate dissociation on wellbore stability, which can help better design drilling muds for ultra deep water operations.

.

DEDICATION

I dedicate this work to my family.

ACKNOWLEDGEMENTS

TABLE OF CONTENTS

LIST OF FIGURES

LIST OF TABLES

1. INTRODUCTION: PROBLEM OVERVIEW

1.1   Drilling through gas hydrates problem overview

Natural gas hydrates are ice-like deposits, containing a mixture of water and gas with methane as a primary gas, which are stable under high pressure and low temperatures and found in deepwater settings at relatively shallow depths below the seafloor and in permafrost regions (Sloan 1998). Reduction in pressure or increase in temperature, as well as use of inhibitors, causes dissociation of gas hydrates. When hydrate-bearing sediments (HBS) are drilled through, a change in pressure and temperature of the sediments may destabilize the hydrates.

Usually, hydrates are found in shallow sediments above the surface casing point and are drilled through before the blowout preventer is installed. Under certain conditions, hydrate dissociation in the formation can lead to problems with wellbore stability and interference with seabed installations, and adversely impact on the efficiency and safety of drilling operations.

There are two main problems associated with gas hydrates dissociation that may lead to wellbore instability:

_____

This thesis follows the style of *SPE Journal.*

a) Dissociation in the wellbore may result in gasification of the drilling fluid, which leads to the lowering of the mud density and changes mud rheology, lowering hydrostatic pressure and further dissociation. This may lead to hole enlargement and wellbore collapse.

b) Dissociation in the HBS may result in change of mechanical and petrophysical properties of the sediments such as increase in permeability and reduction in strength of the sediments.

Prediction of the hazards described above may be achieved by the use of a numerical mechanical-thermal-chemical stability modeling tool that incorporates time-dependency.

HBS have been drilled successfully in the past, but there have been cases of blowout due to hydrate dissociation reported in the literature. As drilling operations move into ever deeper waters, engineers will have to develop a sound understanding of gas hydrate drilling-related threats (Schofield 1997) and identify ahead of time what problems are likely to occur and which steps are necessary to prevent them. Some of the techniques adopted so far to avoid the risks of drilling in HBS include (Freij-Ayoub et al. 2007):

- Cooling the drilling fluid.
- Increasing the mud weight to stabilize the hydrates, but avoiding fracturing the HBS.

- Adding chemical inhibitors and kinetic additives to the drilling fluid to prevent hydrate formation and to reduce hydrate destabilization in the formation.

- Accelerating drilling by running casing immediately after hydrates are encountered and using a cement of high strength and low heat of hydration.

Numerical simulation of the mechanisms leading to wellbore instability in HBS can be an effective tool to assess the allowable drilling parameters such as mud weight, composition and temperature to stay within a safe operational envelope. Some of the factors that need to be evaluated are (Freij-Ayoub et al., (2007):

- Effect of drilling fluid on heating the formation and changing the stresses and pore pressure.

- Effect of heat on the formation's thermodynamic stability of the hydrates and wellbore stability.

- Effect of reduction in HBS strength and loss of cohesion due to hydrate dissociation.

Therefore, modeling wellbore stability in HBS requires consideration of various mechanisms:

- Heat and fluid transport between the drilling fluid and the formation, mechanical deformation, and drilling fluid/formation interaction during drilling process.

- Kinetic rate or equilibrium relations for gas hydrate dissociation/reformation with changes in pressure and temperature.

- The resultant changes in the mechanical and petrophysical properties of HBS

- A representative constitutive equation and yield criterion for the mechanical behavior of HBS of various hydrate concentrations.

1.2   Background

Research to date has presented the numerical description of HBS behavior under changing pressure and temperature. Tsypkin (2000) considered the formation of ice upon hydrate dissociation. Yousif et al. (1991) developed a 1D model for the kinetics of hydrate dissociation in porous media under depressurization using the Kim-Bishnoi scheme (Kim et al., 1987) for the rate of gas generation. The model solved continuity equations for each of the three phases (gas, liquid and hydrates) and used relations between the saturations of the phases and the rates of mass transfer of the phases.

 Darcy's law was used to model the flow of water and gas separately, while porosity and permeability were updated as dissociation took place. Heat transfer was not considered in the aforementioned models. Moridis (2002) developed a numerical model to simulate the kinetic or equilibrium dissociation of gas hydrates with heat transfer and multiphase fluid flow in porous media. This approach does not account for the

mechanical deformation of HBS during hydrate dissociation as the porous medium is assumed to be rigid.

Freij-Ayoub et al. (2007) used numerical modeling to quantify the risk of drilling through HBS when the drilling fluid is at a higher temperature than the formation. The model couples the mechanical deformation of HBS to hydrate dissociation, and assumes thermodynamic equilibrium between the hydrates and the liquid in the pore space. Darcy's law is used to model the fluid flow, which is referred to as 'pseudo-multiphase flow', in that the fluid is assumed to have the properties of the liquid, but pressure contribution also comes from gas liberation.

Most of the publications to date focus on the investigation of mechanical instability of the wellbore caused by cementation loss and modulus reduction due to hydrate dissociation. This work looks into ways to estimate the dissociation process itself more precisely.

In previous work (Amodu, (2008), the changes in drilling mud parameters when HBS are penetrated were analyzed by considering the drilled volume or 'crushed zone' to assess the amount of dissociated hydrates, but potential dissociation further into the formation was not considered.

The black dot shown on Fig. 1.1, which depicts how mud weight is affected by the circulation rate for various rates of penetration, is the initial mud density before the hydrate zone is drilled into. Once the hydrate zone is penetrated, the mud density changes as expected as hydrate dissociates and gas mixes with the mud.

The work by Amodu ((2008) provides estimates of the amount of gas evolved from dissociation in the "crushed" zone only, so this current work expands the investigation zone further into the formation to include the amount of gas that may evolve due to the advancement of the temperature front through the HBS.

A new procedure is proposed that allows quantification of possible dissociation of hydrates in HBS and the effect on the drilling process more accurately.
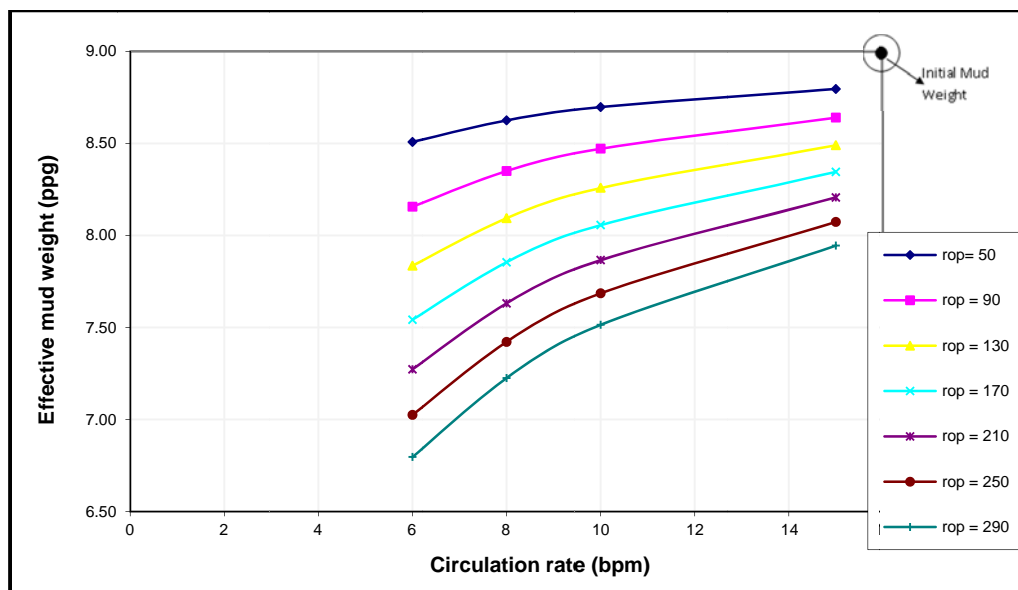
Fig. 1.1—Prediction of mud weight as a function of circulation rate for various rates of penetration

A semi-analytical model was used to estimate the dimensions of the hydrate-bearing layer where the initial pressure and temperature can change while drilling. The dimensions were subsequently used to build a numerical model to simulate the

dissociation of gas hydrate in the layer. The BHP and formation properties were based

on a real field case. The temperature data obtained from Logging-While-Drilling (LWD)

(IODP 2009) did not have the precise temperature measurements of the mud at the bit, as

the tool was located several feet above the bottom of the drillstring. Thus, the

bottomhole temperature (BHT) was calculated numerically, according to the model

proposed by Keller et al. (1973). Some reasonable assumptions were made to simulate

heat transfer and flow in porous media and in the wellbore:

1. Darcy's law is valid in the simulated domain under the conditions of the study.
2. In the transport of dissolved gases and inhibitors, mechanical dispersion is small
   compared to advection (neglecting mechanical dispersion significantly reduced
   memory requirements and execution times).
3. The compressibility and thermal expansion of hydrate are the same as those of
   ice (necessitated by lack of data on the subject).

To mimic the dynamic advancement of drilling, a progressive increase of well

depth was modeled via a change in pressure and temperature conditions in the wellbore,

by discretizing the system in time and space. A minimum time step was chosen to allow

the assumption of steady- state conditions during the selected time period.

2. THESIS STRUCTURE

2.1   Objective

The objective develop a comprehensive and rational algorithm based on existing mathematical and numerical models for risk estimation of drilling through hydrate-bearing sediments.

2.2   Procedures

Below is the list of procedures that I have developed to achieve the objective of my research study.

1. Identify all the physical and chemical phenomena that can take place during drilling through gas hydrate-bearing layers.
2. Divide the whole problem into sub-problems according to regions and correspondent processes. For example: reservoir zone, wellbore zone. Assign correspondent processes to each zone.
3. For the wellbore zone and for the selected mathematical model, develop a code with numerical model capabilities. This model should calculate appropriate bottomhole boundary conditions that will be used in the reservoir model. At this point also identify all the necessary inputs for calculations.
4. Find and put together all the necessary inputs for the wellbore model.
5. For the reservoir zone, start with the simpler case: analytical models in one dimension. Put all the equations of mass and energy balance together.

6. For the reservoir zone and selected mathematical model, write a code with analyticalcapabilities. Identify all the necessary inputs for calculations.

7. Find and put together all the necessary inputs for the reservoir model.

8. At this point specify all the assumptions made.

9. Using the existing analytical model, determine the size of the reservoir that will be affected by drilling. These numbers will be used as inputs for the selected numerical model.

10. Put together all the necessary inputs (including the ones described in Step 9) for the selected reservoir numerical simulator with capabilities of simulation of gas hydrate dissociation.

11. Using the numerical simulator for the reservoir zone, determine the amount of gas that is possible to dissociate and dissolve in the column of drilling mud during the time thathydrate-bearing layer is drilled through.

12. Include the amount of gas that will dissociate from the "crushed" zone.

13. Analyze and conclude whether the amount of gas evolved from hydrate dissociation is capable of causing damage to the wellbore.

2.3　　Approach

There are two main problems associated with gas hydrates dissociations that may lead to wellbore instability:

a) Dissociation occurred in gas-hydrate-bearing sediments may result in change of mechanical and petrophysical properties of the sediments: increase in permeability, reduction in modulus, strength reduction of the sediments.

b) Dissociation occurred in wellbore may result in gasification of the drilling fluid which leads to the lowering of the mud density hence the lowering hydrostatic pressure and further increase of dissociation. This may lead to hole enlargement an wellbore collapse.

Prediction and probability assessment of hazards, described above may be fulfilled through numerical mechanical-thermal-chemical stability modeling tool for time-dependent stability analysis.

As it is common for any modeling process, it will be advantageous to start with simplified cases where number of variables is minimized, allowing important factors to be estimated first.

Also it's reasonable to consider description of the occurring phenomena separately in sediments , at the bit and in the wellbore, to combine their influence on one another in future.

For gas hydrate-bearing sediments, following processes should be described:

- heat transfer between the drilling fluid and the formation.
- kinetic rate of GH dissociation with the change of p/T and resultant changes in mechanical and petrophysical properties of the sediments.
- formation mechanical behavior.

Following assumptions and simplifications may be reasonable at the very beginning:

1. Linear (radial) heat transfer

2. Average constant heat transfer coefficient

3. Approximate distance to the boundary of "transition" zone, where dissociation of GH is initiated by pressure and temperature change.

4. Statical (fixed) dissociation: bottomhole parameters (p_{wf}, T_{wf}).

5. Constant GH-bearing formation thickness

Necessary input data include:

1. formation depth and geothermal coefficient

2. mud p/T at the bottom

3. initial formation conditions (p_i, T_i)

4. GH stability range for p/T

The output parameters will define "transition" zone, i.e. how far in the reservoir the dissociation will possibly occur, or whether it is likely to occur at all. This will allow estimating the amount of gas dissociated in the formation along with the change in mechanical and strength properties of the rock.The phenomena caused by bit interaction with the formation rock should be taken into account as well:

a) mud heating due to friction

Initial data required:

1) approx friction coefficient (rock properties, bit characteristics)

2) mud physical properties

b) amount of cuttings produced from the "crushed" zone per unit of time

Initial data reqired:

1) mechanical properties of the rock

2) bit parameters

To quantify the amount of hydrates that can dissociate in the wellbore we are to analyze parameters change of multiphase solution of drilling mud, cuttings and possible gas + water dissolved from hydrate. Based on the studies of thermo-mechanical coupled model it will be possible to make certain recommendations for drilling parameters and mud properties.

2.4 Structure

In the main part of thesis first, I introduce the field data that were used in calculations for analytical hydrate dissociation model, downhole temperature estimations and numerical simulator for hydrate dissociation. Further, theory, justification of choice, calculations and results with discussions for each model or software that has been used are presented. Finally, discussed results are summarized in conclusion and suggestions for further research were made.

3. FIELD DATA FOR CALCULATIONS

3.1   Review of the available database

Although up till today numerous cases of drilling through gas hydrate-bearing formations are encountered, there is not much data available.

The *Integrated Ocean Drilling Program* (IODP) is an international marine research program that explores Earth's history and structure recorded in seafloor sediments and rocks, and monitors subsea floor environments.

One of the main purposes of expeditions within IODP follows the goals for gas hydrate drilling as proposed by the ODP Gas Hydrates Program Planning Group:

- Study the formation of natural gas hydrate in marine sediments.

- Determine the mechanism of development, nature, magnitude, and global distribution of gas hydrate reservoirs.

- Investigate the gas transport mechanism, and migration pathways through sedimentary structures, from site of origin to reservoir.

- Examine the effect of gas hydrate on the physical properties of the enclosing sediments, particularly as it relates to the potential relationship between gas hydrates and slope stability.

- Investigate the microbiology and geochemistry associated with hydrate formation and dissociation.

The objectives of such expeditions are to test gas hydrate formation models and constrain model parameters, especially models of hydrate concentration through upward

fluid and methane transport. These objectives require (1) high-quality data on the vertical concentration distributions of gas hydrate and free gas and variation landward in the accretionary prism and (2) estimates of the vertical fluid and methane fluxes through the sediment section as a function of landward distance from the deformation front.

All the data are available online at www.iodp-usio.org and can be accessed without restrictions.

IODP Expedition 311 cored a transect across the Cascadia margin off Vancouver studying gas hydrates. At all 5 sites, the first hole (A-hole) drilled was with an MWD/LWD string. The shipboard results, including logging and the mechanical rock property data measured shipboard, as well as an operational summary for each site, are located at http://publications.iodp.org/proceedings/311/311toc.htm.

Data on the hole U1325A are used as a reference for the calculations, as it has the widest set available.

Some important information on site U1325 is provided below including Table 3.1:

Expedition: 311

Location: Cascadia Margin (NE Pacific)

Water Depth (as seen on logs): 2203 mbrf

Total penetration: 350 mbsf

Table 3.1—Site U1325 data

Thermal cond. of sediments	1.1	w/(Mk)
Thermal gradient	0.06+/-0.003	degC/m
Seafloor intercept	3.03+/-0.55	degC
Depth of GHSZ	275+/-25	mbsf
Methane content	89+/-3	%
Hole depth	2212	mbrf
ROP	25-30	m/h
RPM	60	rpm
Porosity at 300 mbsf	45- 55	%
Mud circulation rate	290	gpm
Water Saturation at HBZ	40	%

3.2   Logging tools

The logs were recorded using the LWD/MWD (Logging-While-Drilling/Measurement-While-Drilling) technique, which allows the acquisition of open-hole logs using instruments that are part of the drill string itself. The advantages of this technique include being able to log in formations that would not provide a stable hole for wireline logging (e.g. the upper section of sedimentary formations) and logging a hole immediately after it is drilled, so that it is in good condition and largely free of wash-outs.

The following LWD/MWD services were employed in Hole U1325A: GeoVision (RAB resistivity and gamma ray), EcoScope (ARC resistivity, density, porosity, geochemistry, gamma ray, temperature, and pressure), SonicVision (velocity)

TeleScope (real time transmittal of data to the ship (MWD)), ProVision (NMR magnetic resonance, porosity, bound fluid volume), ADN Vision (ADN density, porosity, caliper).

In Hole U1325A, the rate of penetration was approximately 30 m^3/hr. The drilling fluid was sea water. The well is openhole with some washouts between 0-20 and 270-305 mbsf, but otherwise the hole is generally in-gauge.

3.3   Data processing

The original logs have been depth shifted to the sea floor (-2203 m). The sea floor depth was determined by the step in gamma ray and resistivity values at the sediment-water interface.

Processing of the data is performed in real-time onboard by Schlumberger personnel. Gamma Ray data is measured as Natural Gamma Ray (GR): the GR is normally corrected for hole size (bit size), collar size, and type of drilling fluid. Comparison between gamma ray data collected in LWD and wireline holes during Expedition 311 shows that the former have a much higher value range than the latter. Because the GR value range from the wireline holes appears to be the one expected for these lithologies and is in agreement with the data acquired in ODP Leg 146, the LWD GR is currently under investigation, to assess the cause of such discrepancy. Caution is therefore suggested in interpreting the LWD GR data.

3.4   Downhole temperature and pressure measurements

For the hole U1325A downhole temperature and pressure was measured during MWD and LWD operations. Particularly temperature was measured with Schlumberger EcoScope tool, which is placed 10-15 feet above the bit. Knowing local geothermal gradient and thermophysical properties of hydrate-bearing layer, we were able to predict temperature of drilling mud at the bit with SPT Group Drillbench software. Results presented in Section 4.

The apparent geothermal gradient for studied region is shown on Fig 3.1. The stability boundary for gas hydrate at hydrostatic pressure is shown (calculated using CSMHY; Sloan, 1998) for the background salinity of pore water near the base of the gas hydrate stability zone (GHSZ) at this site, which was similar to seawater (3.5% NaCl). The bottom-simulating reflector (BSR) is predicted from seismic data. The base of the GHSZ is predicted from the thermal gradient.
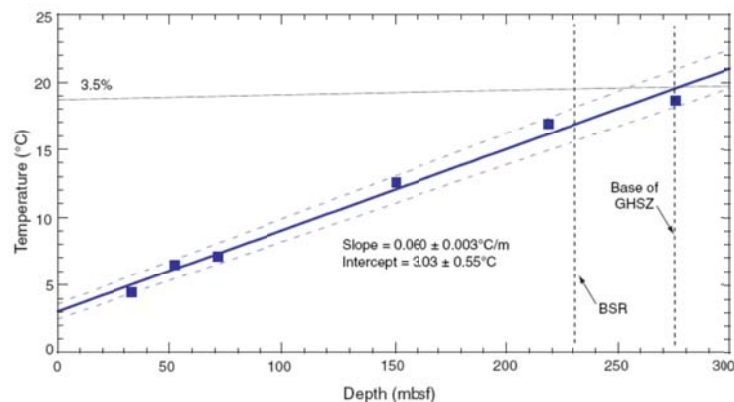

Fig. 3.1—Apparent geothermal gradient at site U1325

Table 3.2 presents summary of parameters that were available at IODP database and were used for numerical simulation.

Table 3.2—Parameters for numerical simulation

Model parameters	Parameter Value	Units
Initial sediment porosity	0.49	
Sediment porosity after hydrate formation	0.25	
Thermal conductivity	1.4	$Wm^{-1}K^{-1}$
Specific heat capacity	1.90E+03	$JK^{-1}kg^{-1}$
Saturated sediment density	2.2	g/cm^3
In situ pore pressure	17	Mpa
Mud pressure	20.967	MPa
In situ temperature	15	°C (288 K)
Drilling mud temperature	20	°C (293 K)
Intrinsic permeability	1.00E-15	m^2
Hydrates crystal volume	1.73E-27	
Cohesion	1.8	MPa
Angle of internal friction	35	°
Tensile strength	1.5	MPa

4. LINEAR 1D HYDRATE DECOMPOSITION FOLLOWING PRESSURE DROP

4.1 Model theory

The proposed model is shown in Fig.4.1, where free gas (m(1-β)) and hydrate (mβ) coexist in the pore space of a layer at time zero, corresponding to pressure (P_e) and temperature (T_e) where m is the porosity and β is the hydrate saturation in the layer. Subsequently, the pressure at the wellbore (x=0) sharply drops to a value $P_G < P_D < P_e$, where P_D is the hydrate dissociation pressure at the specified layer temperature. The pressure is then gradually decreased and two zones of gas filtration appear with different collector properties, separated by moving boundary l(t). The surface l(t) is the boundary between the zone where dissociation start (zone 1) and the zone where conditions are still within the hydrate stability region (zone 2).
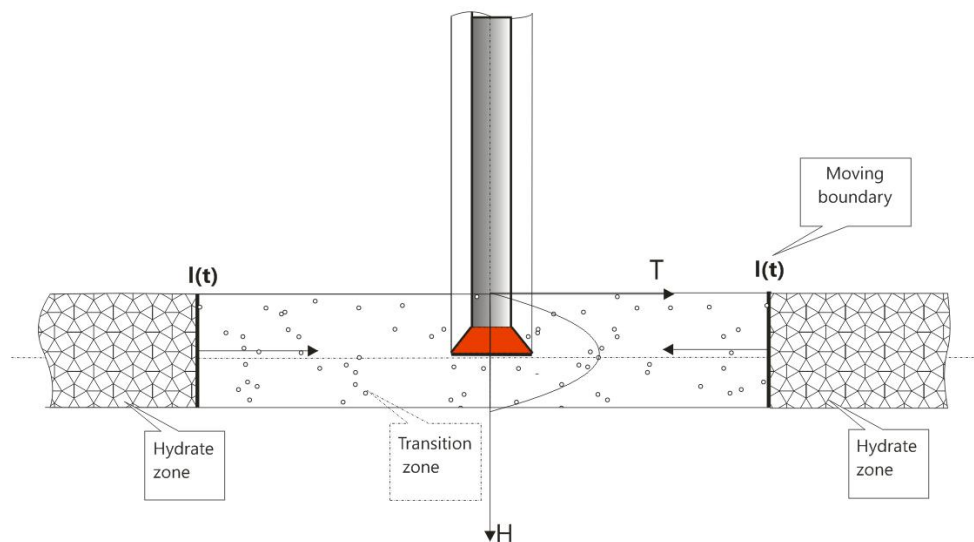

Fig.4.1—Schematic of gas hydrate dissociation for a simple 1D model

During dissociation of hydrates at surface, water is released along with gas. It is assumed that the permeability to water is zero, so this phase movies immobile and, when released at l(t), it decreases porosity and gas permeability in the first zone. Filtration of gas occurs in a direction towards a wellbore, while the surface l(t) moves further into reservoir. The pressure distribution in the layer is described by the following gas filtration equation (Makogon 1997):

$$\frac{2m_n\mu_n}{k_n}\frac{\partial P_n}{\partial t} = \frac{\partial^2 P_n^2}{\partial x^2};$$

(1)

μ = viscosity

K = permeability

P = pressure

$m_1 = (1-\sigma)m$, where σ- water content of pores.

$m_2 = (1-\beta)m$;

Subscript 'n' denotes zone 1 or zone 2

The temperature of a gas saturated layer can be described by considering the convective and conductive heat flows, throttling and adiabatic effects (Makogon 1997):

$$a_n\frac{\partial^2 T_n}{\partial x^2} = \frac{\partial T_n}{\partial t} - \frac{\rho_C k_n}{\alpha_n\mu}\frac{\partial P_n}{\partial x}\left(\frac{\partial T_n}{\partial x} - \delta\frac{\partial P_n}{\partial x}\right) - \eta\frac{m_n\rho_C}{\alpha_n}\frac{\partial P_n}{\partial t};$$

(2)

where:

a = is the thermal conductivity;

α = is the heat capacity;

ρ_c = is the volume heat capacity of gas;

δ = is the throttling coefficient of gas;

T = temperature at the point of interest..

η = is the adiabatic coefficients of gas.

Assuming $a_n = 0$ (i.e. the conductive heat flow in the porous medium is several orders of magnitude less than the convective flow), the following boundary conditions can be used:

$$T_2(\infty, t) = T_2(x, 0) = T_e,$$
$$T_1(l(t), t) = T_2(l, t);$$

The solution of the general equation for temperature field distribution is (Makogon 1997).

$$T_1 = T_D + A_1\delta\left[\text{erf }\lambda_1 - \text{erf }z_1 + \left(1 + \frac{\eta}{\delta}B_1\right)(\Phi_1(z_1) - \Phi_1(\alpha_1))\right];$$
$$T_2 = T_e + A_2\delta\left[\text{erf }z_2 - \left(1 + \frac{\eta}{\delta}B_2\right)\Phi_2(z_2)\right];$$

(3)

where:

$$A_1 = \frac{2}{erf\lambda_1}\frac{P_D^2 - P_G^2}{P_G}; \quad A_1 = \frac{2}{erf\lambda_2}\frac{P_e^2 - P_D^2}{P_e};$$

$$\Phi_1(\xi_1) = \frac{2}{\sqrt{\pi}} \int_0^{\xi_1} \frac{\eta e^{\eta^2} d\eta}{\eta + C_1 e^{-\eta^2}};$$

$$\Phi_2(\xi_2) = \frac{2}{\sqrt{\pi}} \int_{\xi_2}^{\infty} \frac{\eta e^{\eta^2} d\eta}{\eta + C_2 e^{-\eta^2}};$$

$$B_1 = \frac{1}{4} \frac{P_G^2 m_1 \rho_{0C}}{P_0 \alpha_I};$$

$$B_2 = \frac{1}{4} \frac{P_e^2 m_2 \rho_{0C}}{P_0 \alpha_{II}};$$

$$C_1 = \frac{P_D^2 - P_G^2}{P_G} \frac{\rho_{0C}}{\alpha_I} \frac{1}{2\sqrt{\pi} \operatorname{erf} \lambda_1} \frac{k_1}{\mu \chi_1};$$

$$C_2 = \frac{P_e^2 - P_D^2}{P_e} \frac{\rho_{0C}}{\alpha_{II}} \frac{1}{2\sqrt{\pi} \operatorname{erf} \lambda_2} \frac{k_2}{\mu \chi_2};$$

$$\lambda_n = \frac{x}{2\sqrt{\chi_n t}};$$

$$\alpha_n = \sqrt{\frac{\gamma}{4\chi_n}};$$

$$\chi_1 = \frac{k_1 P_G}{m(1-\sigma)\mu};$$

$$\chi_2 = \frac{k_2 P_e}{m(1-\beta)\mu};$$

$$\operatorname{erf} \xi = \frac{2}{\left(\sqrt{\pi} \int_0^{\xi} e^{-\eta^2} d\eta\right)};$$

$$\operatorname{erfc} \xi = 1 - \operatorname{erf} \xi;$$

P_D = dissociation pressure,

P_G = BHP,

P_e - initial formation pressure,

P_0 - surface pressure,

ρ_{0C} - volume heat capacity of gas at surface conditions,

α_I, α_{II} - heat capacity of 1st and 2nd zone correspondingly.

z_1, z_2 - function arguments, substituted by correspondent value s of α_1, α_2 (see below)

To determine dissociation pressure, P_D, an empirical equation is used (Makogon, 1997):

$$logP_D = a(T_D - T_0) + b(T_D - T_0)^2 + c \tag{4}$$

where:

a, b, c = are empirical constants depending on hydrate composition and the interval of pressure and temperature variation.

The temperature of hydrate decomposition is determined when $z_2 = \alpha_2$ using equation for T_2 (Makogon, 1997):

$$T_D = T_e - A_2\delta \left[erfc \, \alpha_2 - \left(1 + \frac{\eta}{\delta}B_2 \right) \Phi_2(\alpha_2) \right] \tag{5}$$

The parameter γ is determined from equation:

$$k_1 \frac{P_D^2 - P_G^2}{\sqrt{\pi \chi_1}} \frac{e^{-\alpha_1^2}}{\operatorname{erf} \alpha_1} - k_2 \frac{P_e^2 - P_D^2}{\sqrt{\pi \chi_2}} \frac{e^{-\alpha_2^2}}{\operatorname{erf} \alpha_2} = A\sqrt{\gamma}; \tag{6}$$

$$A = \left[\frac{\beta \varepsilon P_0 T_D}{T_0} Z - (\beta - \sigma) P_D \right] m\mu; \tag{7}$$

Production rate of gas per unit length of a gallery is found from the expression:

$$Q = -\frac{kh}{\mu} \frac{\partial P_1(0,t)}{\partial x} = \frac{k_1 h}{\mu} \frac{P_D^2 - P_G^2}{P_G} \frac{1}{\operatorname{erf} \alpha_1} \frac{1}{2\sqrt{\pi t \chi_1}}; \tag{8}$$

Gas rate decreases in time. It depends on the thickness of a layer h and on hydrodynamic and thermodynamic parameters of the first and second regions.

Thus using equation (5) we can determine all the major characteristics of the process gas hydrates decomposition during a pressure drop:

a) distribution of pressure and temperature in a layer

b) temperature

c) pressure

d) rate of hydrate decomposition

e) gas rate

f) water content of a layer during decomposition

4.2   Calculation results for linear gas flow case

An algorithm for calculation of decomposition pressure and temperature has been set up in *Mathematica* software package. Knowing physical and chemical properties of the gas hydrates and initial pressure and temperature, we can calculate decomposition temperature and pressure and temperature propagation into the formation.

Fig 4.2 shows approximate estimation of time when decomposition would take place (approximately 200th minute on the graph). Brown and green horizontal lines define dissociation pressure and temperature respectively for a system considered. Red dots are the measured pressure data and bright-green line is the predicted temperature distribution in the wellbore during the time that the hydrate-bearing layer is drilled through. As we see, temperature never reaches the decomposition temperature level, but pressure is below the hydration formation pressure, decomposition will occur until 200th minute and later, when pressure will be below the brown line once more. Using this graph we can determine start and the end of dissociation process while drilling through hydrate bearing layer.

Analytical model was also used to estimate how far into reservoir the pressure drops during drilling. This estimate allowed to choose appropriate size for the numerical modeling. For the considered hydrate-bearing layer the pressure drop was estimated under drilling conditions as shown on Fig 4.3. Distance into formation, where pressure drops lower than initial pressure, was used as lateral dimension of the numerical model. In this case, pressure stabilizes at 500m, thus the size of a numerical model across X and Y-axis would be 500m.
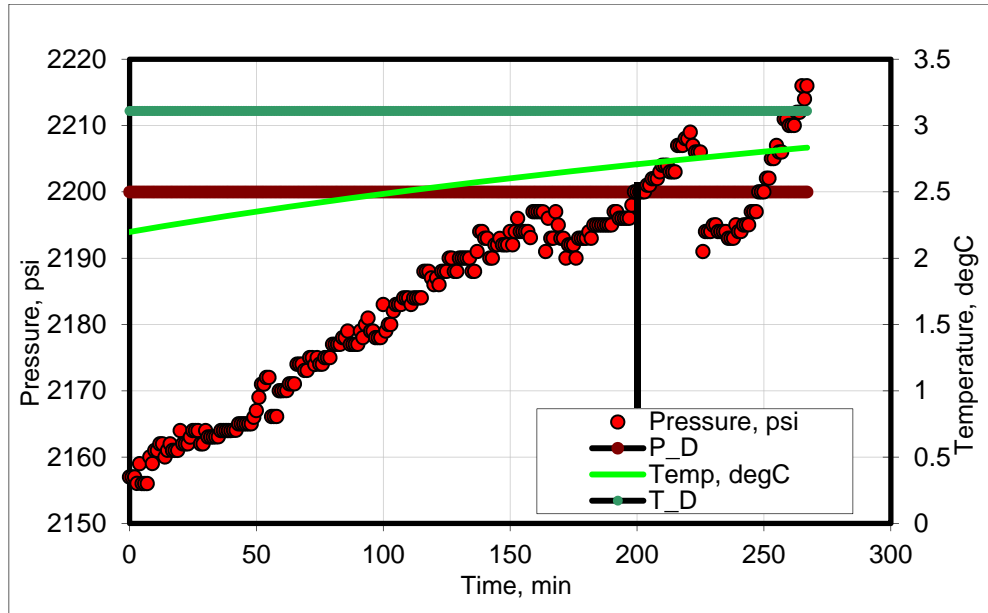
Fig. 4.2—Estimation of drilling time to the moment, when decomposition occurs
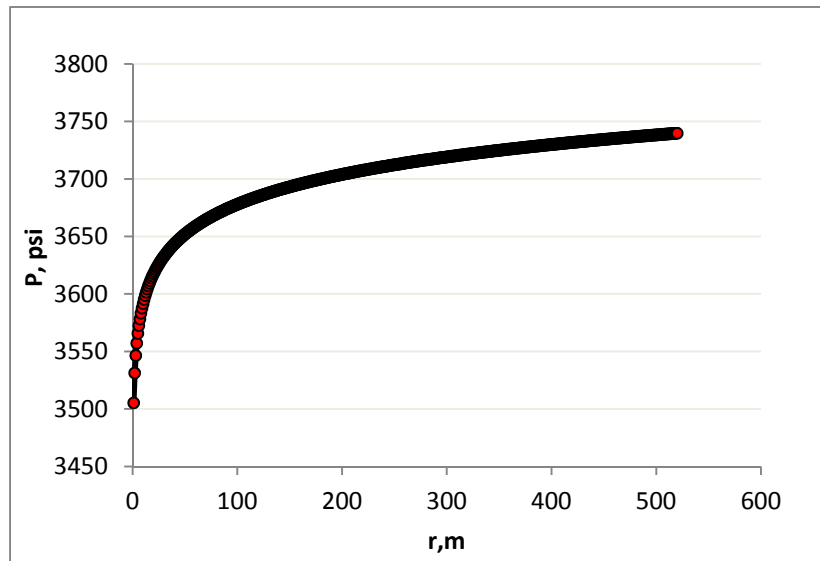

Fig. 4.3—Pressure distribution in the drilled HBS layer estimated with analytical model

5. NUMERICAL SIMULATION OF HYDRATE DISSOCIATION IN HYDRATE-BEARING LAYER

5.1 Determination of boundary conditions

To solve differential equations of fluid flow in the reservoir in case of hydrate dissociation occurs we need to define boundary conditions. While pressure and temperature at the moving front of dissociation are assumed to be constant, temperature and pressure at the wellbore is dynamically changing. Bottomhole pressure is available from MWD data. However, measurements of temperature, which were provided by LWD, were made 30-40 feet above the bit and hence are incorrect.

To define temperature of drilling mud at the bit, SPT Group's Drillbench software was implemented. It differs from the measured values, because the resolution of measurements is 1 degree K, and predicted values are obtained from single numerical model.

SPT Group's Drillbench allows 2D numerical dynamic simulation of wellbore temperature and pressure while drilling. It couples dynamic modeling of wellbore temperatures with dynamic flow modeling, and has been proven to give close to actual results (Fjelde, Arild et al. 2006). Using Drillbench software we were able to account for sources of energy, which are characteristic only to drilling processes, such as heat generated by friction of drillbit and formation, friction of drilling mud in the drillstem and annulus.

Fig 5.1 demonstrates example input window for mud properties in Drillbench Presmod module for simulstion of pressure and temperature distribution in wellbore while drilling.
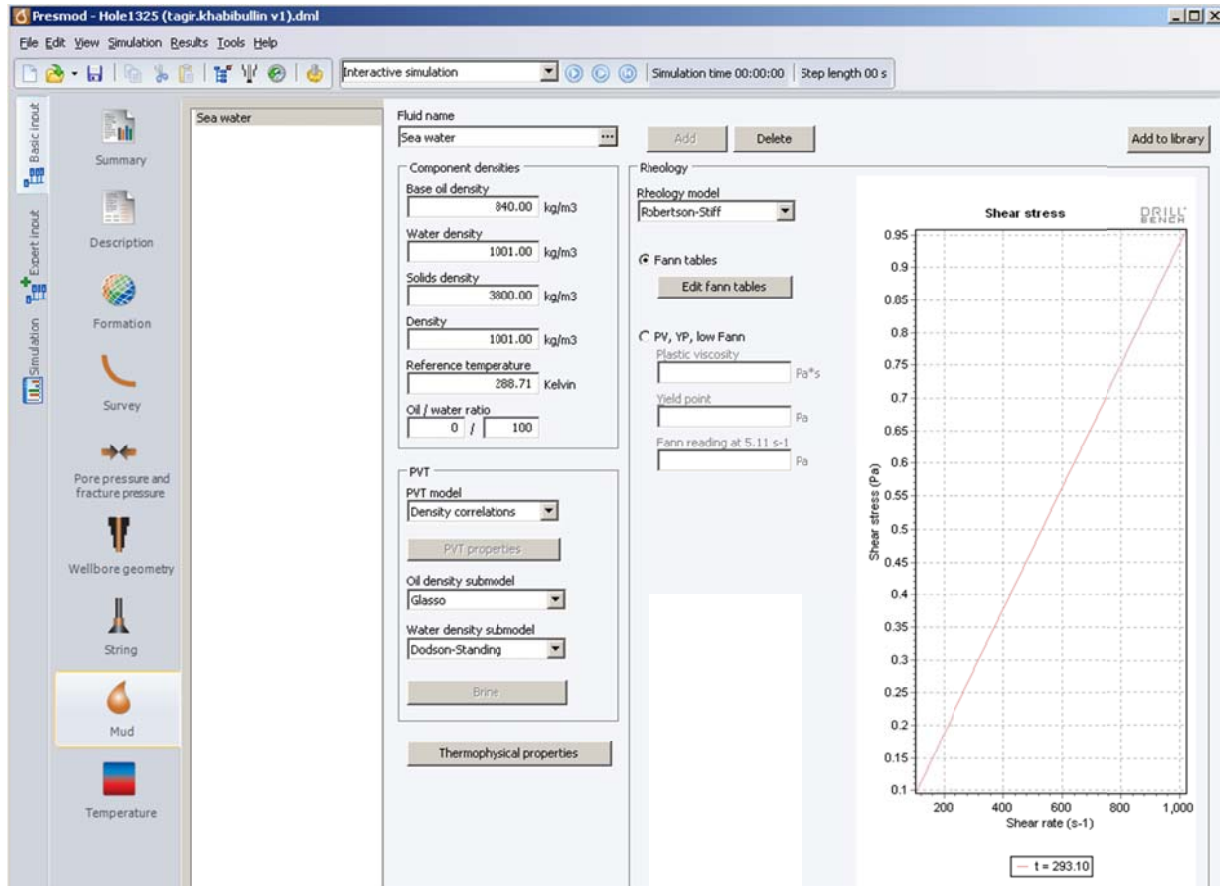
Fig 5.1—Drillbench input window for mud properties

Fig. 5.2 demonstrates wellbore temperature profile for selected interval of drilling. Input data for the simulation run are shown in Table 5.1.
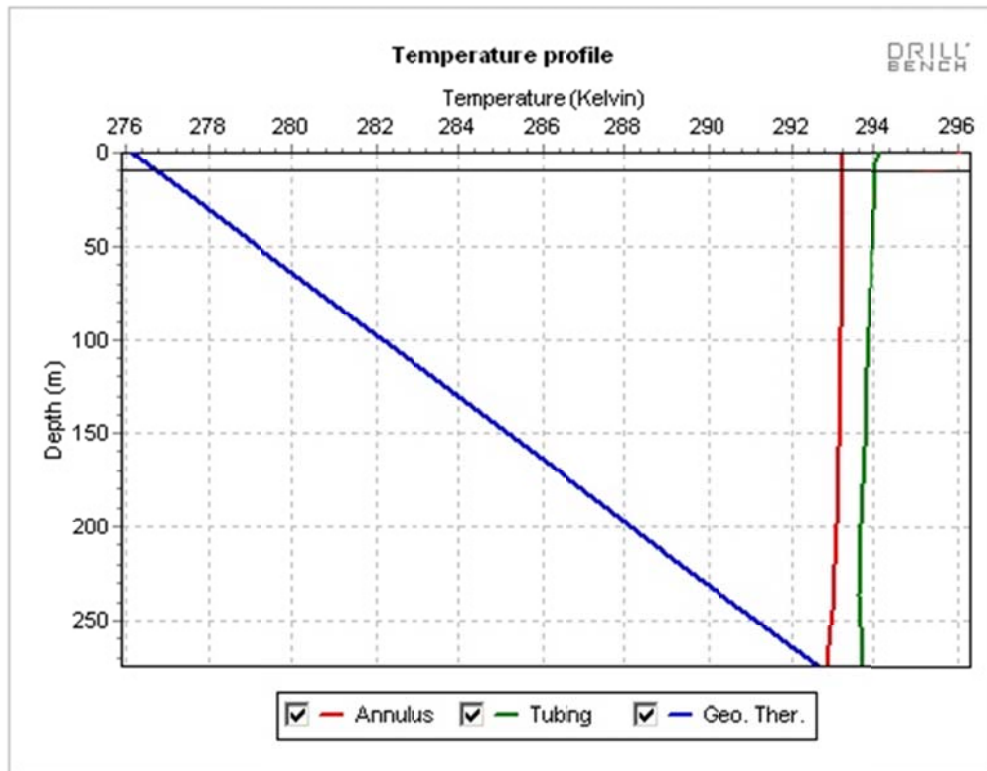
Fig 5.2—Wellbore Temperature profile predicted with Drillbench simulation software

Table 5.1—Hole U1325A data

Thermal conductivity of sediments	1.1	w/(Mk)
Thermal gradient	0.06+/-0.003	K/m
Seafloor intercept	276.03+/-0.55	K
Depth of GHSZ	275+/-25	mbsf
Methane content	89+/-3	%
Water depth	2212	m
ROP	25-30	m/h
RPM	60	rpm
Porosity at 300mbrf	45- 55	%
Mud circ. rate	290	gpm
S_w at HBZ	40	%

It is necessary to mention that Fig 5.2 demonstrates the case, when simulated temperature of the drilling mud in the formation entry point is relatively high (about 22-24°C). Due to the high circulation rate specified for simulation, mud does not cool down significantly. However, in case of riserless drilling in deep, cold waters temperature of the drilling at the sea bottom mud may drop to as low as 2-3°C. In this case, temperature of mud never reaches dissociation temperature of hydrates and in fact appears to be low enough.

5.2   Modeling of drilling through hydrate-bearing layer

We use HydrateResSim reservoir simulation code to model dissociation of hydrate in the hydrate-bearing layer.

HydrateResSim is a code for numerical simulation offluid and heat transport in hydrate-bearing sediments. By solving the coupled equations of mass and heat balance, HydrateResSim can model the non-isothermal gas release, phase behavior and flow of fluids and heat under conditions typical of common natural methane-hydrate. HydrateResSim (HRS) includes both an equilibrium and a kinetic model of hydrate formation and dissociation. The model accounts for heat and up to four mass components, i.e., water, CH4, hydrate, and water-soluble inhibitors such as salts or alcohols. These are partitioned among four possible phases (gas phase, liquid phase, ice phase and hydrate phase). Hydrate dissociation or formation, phase changes and the corresponding thermal effects are fully described, as are the effects of inhibitors. The model can describe all possible hydrate dissociation mechanisms, i.e., depressurization, thermal stimulation, salting-out effects and inhibitor-induced effects.

Although code is aimed for simulation of gas production, it is written in a very generic way, and it is possible with several adjustments to apply it for our case in order to estimate the amount of hydrate dissociated due to pressure depletion and temperature increase.

The assumptions that are made for the code application are as follows:

1) Darcy's law is valid in the simulated domain under the conditions of the study.

2) In the transport of dissolved gases and inhibitors, mechanical dispersion is small compared to advection (by neglecting mechanical dispersion, memory requirements and execution times are significantly reduced).

3) The compressibility and thermal expansivity of hydrate are the same as those of ice (necessitated by dearth of data on the subject).

For the dynamic process of drilling as compared to production from already drilled and completed well we need to account for instantaneous increase of the well depth which means instantaneous change in pressure and temperature in the wellbore.

Pressure change at the bit is caused by increased hydraulic column of mud and changing GLR : $P_{BHP} = f(\rho_{mud}, H, GLR)$. GLR may change due to hydrate dissociation while drilling.

For given moment in time, while the well advances into the formation we are to specify boundary temperature at the wellbore for each vertical segments (gridblock).

As shown in Fig. 5.3, to simplify the problem we can assume constant boundary pressures and temperatures for each vertical segment for the time interval that this segment is being drilled through.

As drilling proceeds deeper into next segment, we recalculate initial conditions at the wellbore and run simulator for a fixed well with increased penetration into the hydrate-bearing zone. In each case we averaged temperature and pressure at the wellbore for each vertical segment.
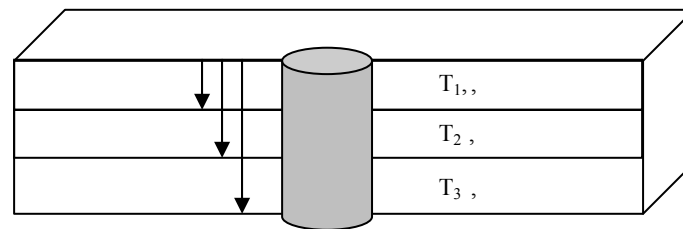
Fig. 5.3—Schematic of vertical discretization of hydrate-bearing layer

As in case of production we can represent dissociation of hydrate while drilling as production of gas from gas hydrate layer with fixed the BHPs to determine rate of dissociation (i.e. production of gas) of gas hydrate into the drilling mud.

5.3   Hydrate- bearing layer representation

Based on analytical model calculations, we determine the dissociation front location and pressure distribution profile for the layer drill-through time, knowing ROP. For the IODP hole U1325A, HBS layer thickness of 45 m and min. ROP of 20m/hr, drill-through time is 1.5 hours After 3.5 hours, estimated with analytical model pressure

distribution is represented on Fig 4.3. With initial pressure Pe = 3749 psi, it can be seen, that pressure distribution stabilizes at 500 m away from the wellbore. As a result, we use 500x500x45 m model with the grid of 100x100x9 blocks to represent the hydrate-bearing layer (Fig. 5.4).
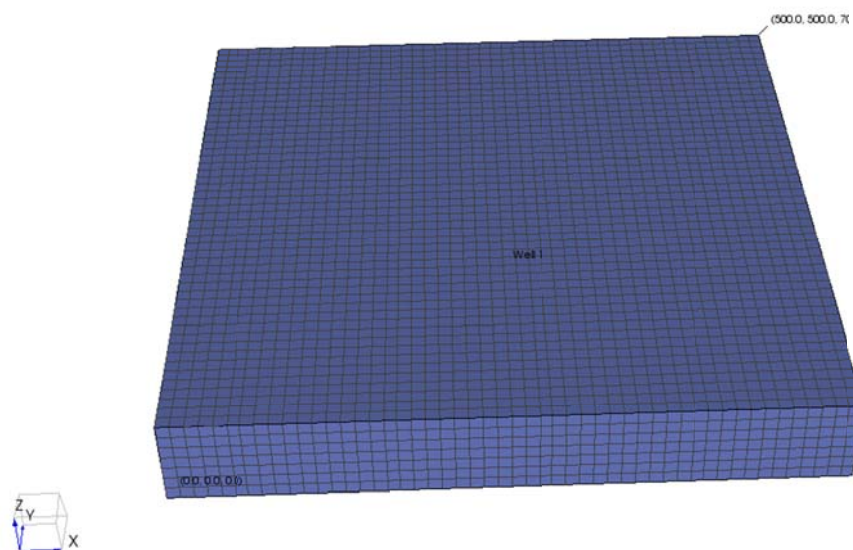
Fig 5.4—Suggested layer model: 500x500x45 m, with 100x100x9 grid

5.4   Calculations for coupled mechanical-thermal transport in HBZ

The well drilling simulated in a formation of the properties in Table 3.2. In the calculation, the formation is impermeable HBS at equilibrium conditions at time $\Delta t=0$. The dissociation process is modeled with thermal transport phenomena. Formation temperature rise slightly increases the pore pressure. The new PT conditions mostly due to the increase in temperature will cause that the hydrates instability.

Figs. 5.5, 5.6 and 5.7 show that hydrates will dissociate in such a region amount by which the pressure increase advances in the formation is dependent on the relative values of the hydraulic and thermal diffusivities. In most cases heat transport will be faster than pressure diffusion, though in a highly permeable formation the reverse could be the case, leading to significant transport of heat by advection (not modelled here). As seen from Fig. 5.5, temperature increase will destabilize hydrates.

As the temperature of the formation increases with time the areas inside the formation to the left of these stability pressure profiles become unstable for the hydrates (if we assume they exist in the sediments).
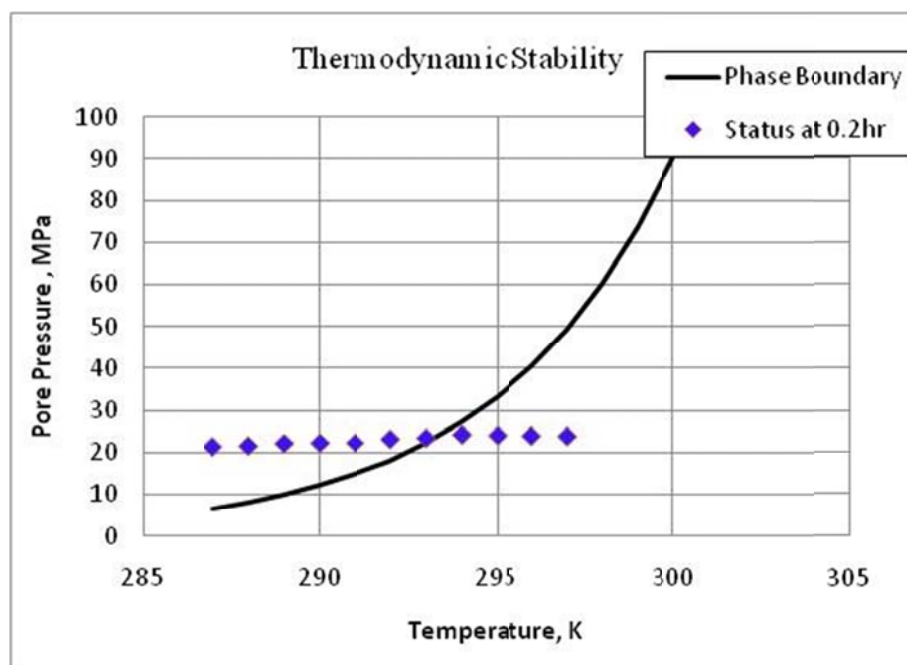
Fig. 5.5—Gas hydrates thermodynamic stability
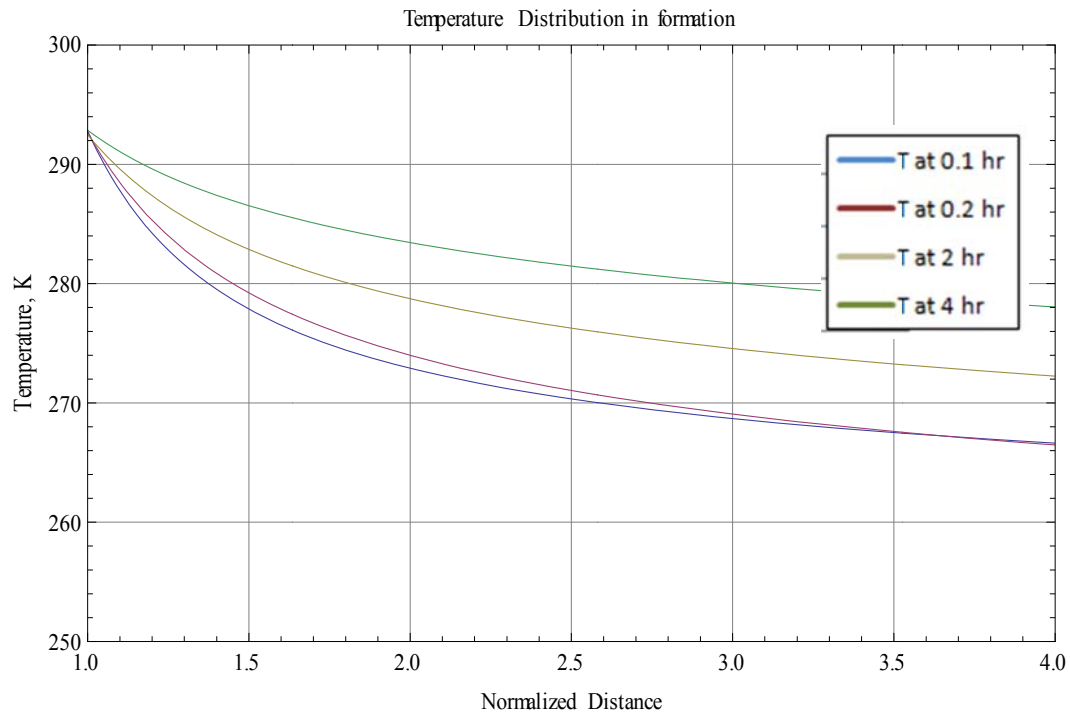
Fig. 5.6—Temperature distribution in formation

Total amount of gas, dissociated due to drilling will be equal to the sum of amount dissociated from the crushed zone and the amount from the advancement of the dissociation front into the formation:

$$Q_t = Q_{crushed} + Q_{advancement}$$

where

$$Q_{crushed} = 2\pi r h * \phi * C_h;$$

where $r-$ wellbore radius, $h-$ thickness of the drilled interval, $\phi-$porosity of the layer, C_h-hydrate concentration.

Amount of gas hydrate dissociated into gas and water from the formation mainly depends on in-situ pressure and temperature. Downhole conditions can be changed by changing drilling parameters such as ROP, ROM, mud temperature, mud density. By lowering the temperature or raising the pressure of mud column we can reduce amount of gas released into the wellbore or avoid dissociation at all.

Several simulation runs were made in order to assess influence of the temperature of the drilling mud or bottomhole pressure on the hydrate dissociation process. Fig 5.7 illustrates the rate of released gas in time. We can see that during drilling through the formation, the rate gradually increases, as expected, because we add more producing layers into our model. When we pass the hydrate-bearing zone, rate starts to decrease, because of cooler drilling fluid above the bit and probably due to reduction in gas relative permeability: water released along with the gas blocks pores. We stop simulation after 3.15 hours- at the moment, when gas rate becomes 0. The presence of mud in the column was simulated by adding heat source.

Graph below (Fig. 5.8) shows that for the case considered, total amount of gas released due to dissociation can be decreased dramatically with lowering temperature by 2K. Fig. 5.9 shows that total amount of gas released due to dissociation can also be decreased with increasing BHP by 1MPa.
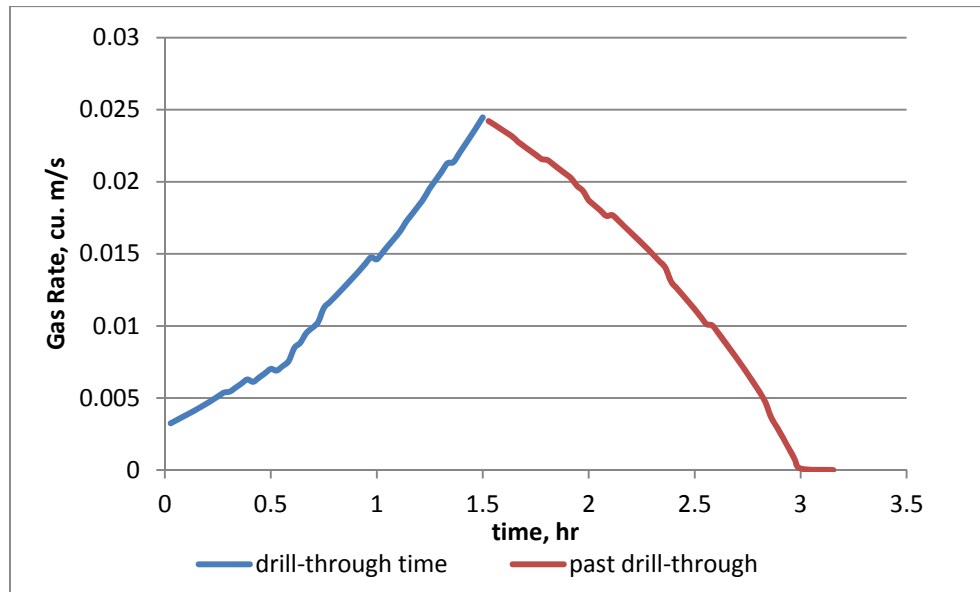
Fig. 5.7—Instantaneous rate of released gas
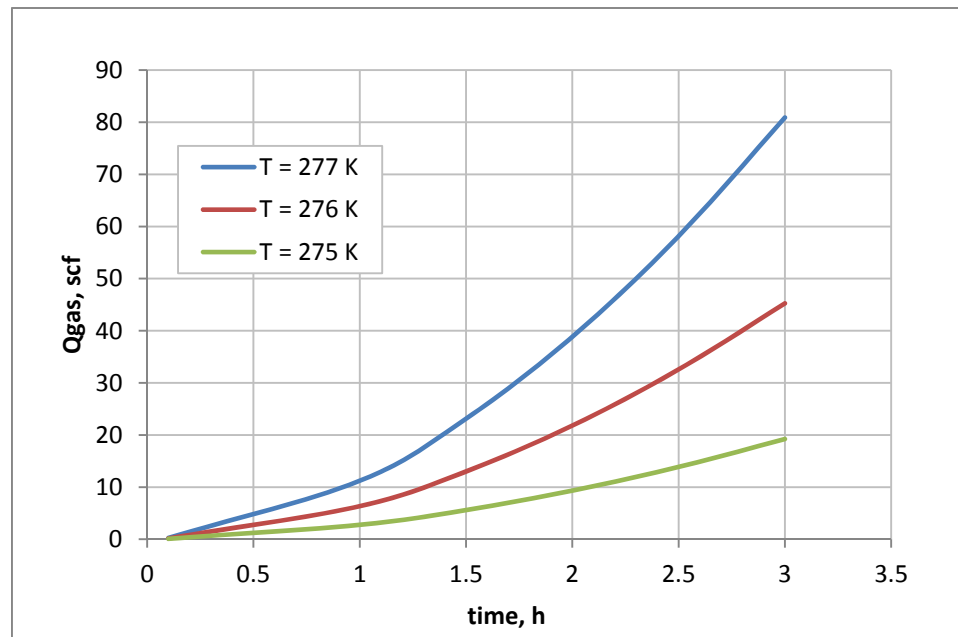
Fig. 5.8—Cumulative Dissociated Gas vs. Time decreases with colder drilling mud
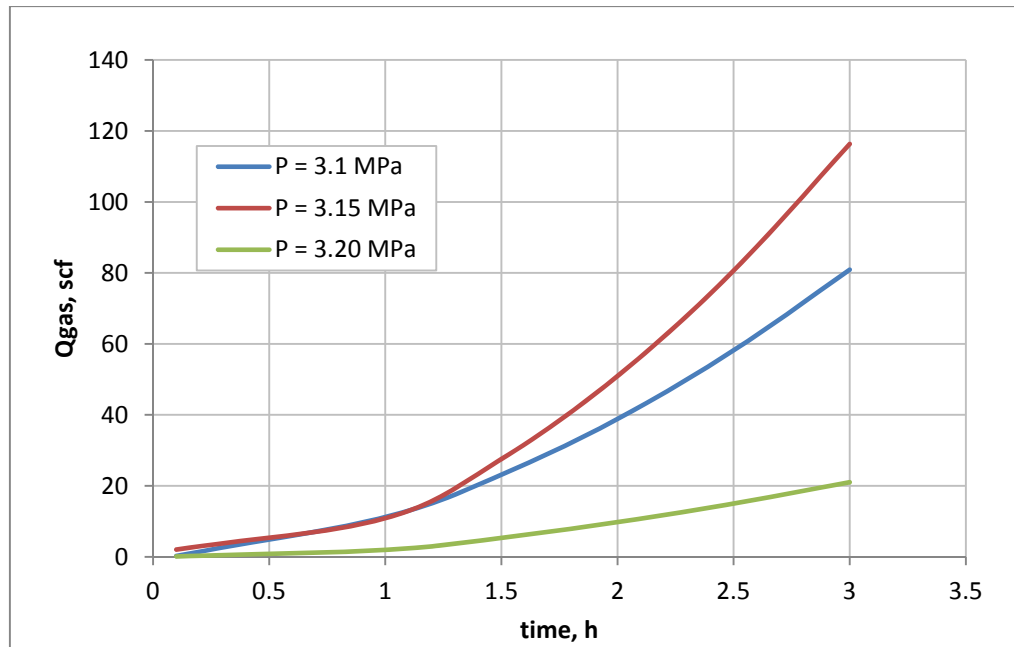
Fig. 5.9—Cumulative Dissociated Gas vs. Time decreases with higher BHP

Depending on the requirements of the drilling program, restrictions on changing of the parameters may apply. For example in case of low fracture pressure, BHP cannot be increased above the fracture limit or temperature of the drilling mud cannot be decreased due to strong dependence of the rheological properties on the temperature.

Based on values of temperature and pressure we were able determine progress of dissociation front into formation. As shown on Fig. 5.10, in our case, dissociation front advances as far as 5.34 m into hydrate bearing layer. This means, that in this radius, hydrates either fully dissociated or just started to dissociate. Dissociation of hydrates changes mechanical properties of the sediment due to reduction in sedimentation (Freij-Ayoub, R., 2007). This could lead to sediment compaction and wellbore collapse.
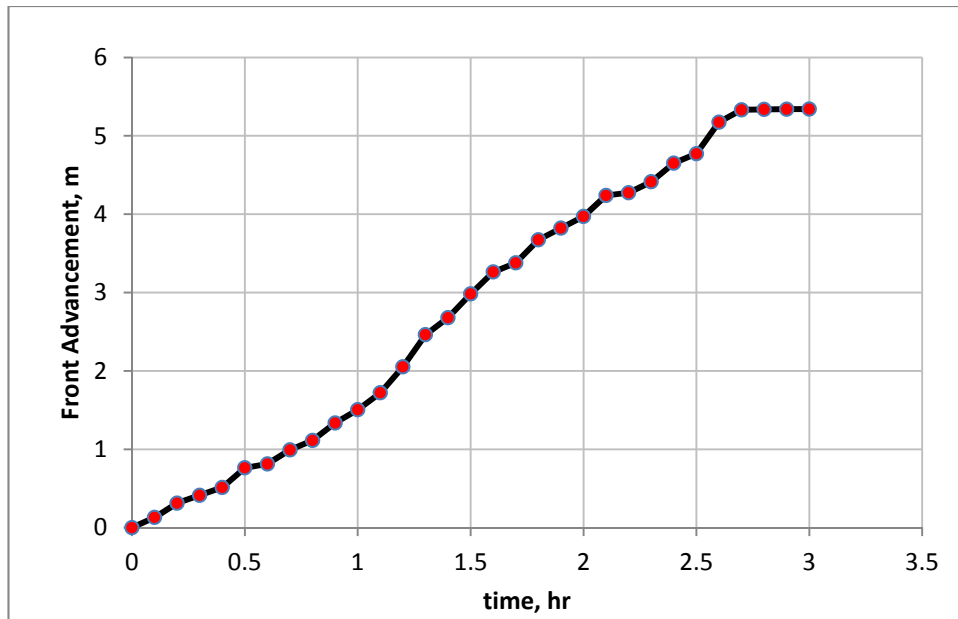
Fig 5.10—Dissociation front advancement

6. RELEASED GAS IN THE WELLBORE

When gas hydrates dissociate in the formation during drilling, gas enters into the mud, decreasing its density, and changing rheological properties. With mud, losing its weight well is at risk of a kick or a blowout.

As stated earlier, in previous work, done by Amodu (2008) only "drilled" amount of gas was taken into consideration. In this work we estimated total amount of gas that was released due to dissociation both from frilled zone and from surrounding formation.

Fig 6.1 shows comparison of amount of gas that was release from the drilled zone and total amount of gas for our case. As expected total amount of gas released exceeds amount of "drilled" gas quite significantly.
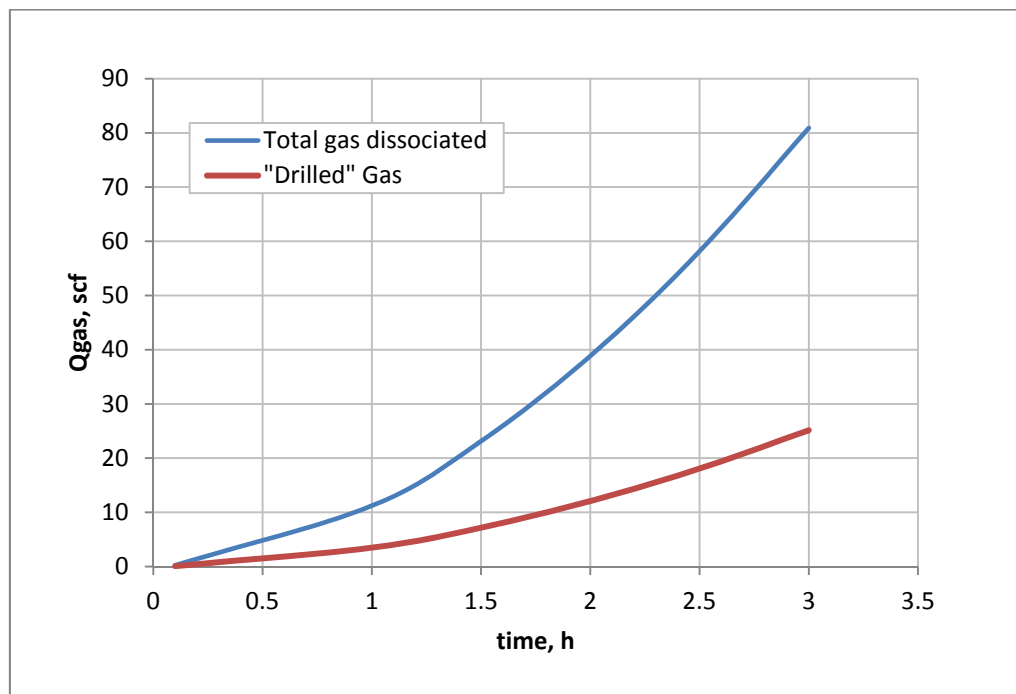
Fig. 6.1—Total gas vs. "drilled" gas released during drilling

To analyze influence of the released gas on the drilling process, we followed the procedure, suggested by Amodu (2008). Knowing the requirements on mud weight, which determined by limits of BHP. For conventional drilling, BHP must be below fracture pressure and above formation pressure.

To determine interval for ROP that will result in optimal mud weight we use correlation between gas/mud ratio and ROP:

$$R = r_m Z \, T_d \frac{q_m}{d_b^2 \phi S_g P_b};$$ (9)

where

R- rate of penetration (m/s)

Z- compressibility factor

T_d-bottomhole temperature

q_m-circulation rate

ϕ-porosity

S_g-gas saturation

P_d-bottomhole pressure

d_b-drillbit diameter

r_m-gas/mud ratio

Fig. 6.2 illustrates approach for selection of optimal ROP based on given circulation rate. The basis for judgment in the above graph is the fracture gradient and

the formation pressure. One of the most important goals in a normal drilling operation is to keep the mud weight between the fracture pressure and formation pressure. The exception to this rule would be in the case where it is desired to drill underbalanced depending on the knowledge, history and goals of the formation. In order to relate the 3 parameters, a suitable hydrostatic gradient is selected based on history, cores or knowledge of formation. This hydrostatic gradient is used in computing the required mud weight in order to keep the formation safe. The required mud weight is shown on Fig 6.2 with the horizontal dark colored line. In this case 935 kg/m^3 is selected.

The goal is to make sure the mud weight is always above 935 kg/m^3 knowing very well it would never exceed 1115 kg/m^3 due to the dissolution of the gas in the drill mud. According the graph, only the shaded part of Fig 6.2 matches this criterion hence the other 2 parameters must be selected to match or fall within this area. This leaves us with only very few possible rates of penetration and circulation rates for this particular example.

The maximum possible ROP would be about 15 m/h for the circulation rates investigated in this work or in order to circulate at 0.004 m^3/s. Since the ROP of penetration is directly related to drilling time which constitutes a major cost of an offshore well, it is important to try to maximize the ROP while keeping all other parameters within the safety limit of the rig, its personnel and the environment in general. Line A in Fig 6.2 shows the maximum possible circulation rate and rate of penetration for the equivalent mud weight selected (935 kg/m^3).
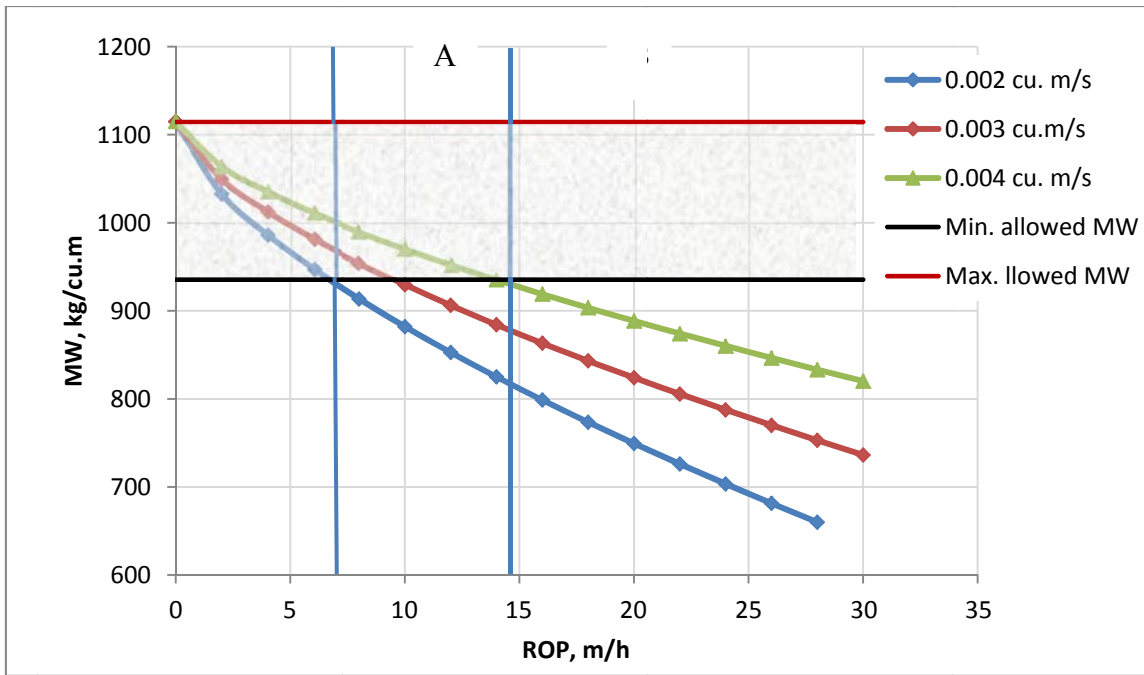
Fig. 6.2—Prediction of variation of mud weight with rate of penetration and circulation rate

7. SUMMARY AND CONCLUSIONS

7.1. Conclusions

Previously published work analyzed changes in drilling mud parameters when gas HBS are drilled through, but only took into consideration the drilled volume, or "crushed zone" for the assessment of amount of the hydrates that are likely to dissociate. The possible further dissociation into the formation was not considered.

A new procedure for estimating the amount of hydrate dissociated during drilling in HBS is presented. A semi-analytical 1D model of heat and fluid transport was coupled with a numerical model of temperature distribution along the wellbore. This combination allowed the estimation of the size of the investigation zone into the hydrate bearing layer and calculated the amount of gas that could be released due to pressure drop or temperature increase while drilling. The effects of variations in porosity and permeability on pressure and temperature profiles and the movement of a dissociation front were studied for a real field case, where the BHP and the formation properties were obtained from a public database, and the BHT was calculated numerically.

The influence of changes in BHT and BHP on the amount of gas released due to hydrate dissociation was investigated. The simulations showed that moderate temperature increase due to drilling process will not affect the gas hydrate dissociation. The main parameters that affect gas hydrate dissociation are drilling mud temperature at the bit and BHP.

The results provide an understanding of the effects of drilling a wellbore through HBS and the impact of the drilling fluid temperature and BHP on changes in temperature

and pore pressure within the surrounding sediments. For each specific case, the amount of gas hydrate that can dissociate will depend significantly on both initial formation characteristics and bottomhole conditions: mud temperature and pressure. The model can provide quantitative results of the impact of hydrate dissociation on wellbore stability, which can help better design drilling muds for ultra deep water operations and so improve their performance in hydrate stabilization.

The proposed workflow has the capability of quantifying the gas-hydrate dissociation processes in sediments with a minimum number of assumptions.

We showed that gas released from dissociation both in the surrounding formation and "drilled" zone, narrows significantly an interval for ROP selection at which drilling operation will be safe.

7.2   Recommendations for future work

In this work we estimated the amount of gas, that would be released into drilling mud due to dissociation of hydrates during drilling operations. Logical continuation of this work would be quantitative study of all available methods that would prevents hydrates from dissociation and building an algorithm that would allow to choose the best or optimal method for a particular well in a particular location.

REFERENCES

Amodu, A. 2008. Drilling Through Gas Hydrates Formations: Possible Problems and Suggested Solution. MS Thesis, Texas A&M University, College Station, Texas.

Apak, E. C. and E. M. Ozbayoglu 2009. Heat Distribution Within the Wellbore While Drilling. *Petroleum Science and Technology* **27**(7): 678 - 686. doi:10.1080/10916460802105617.

Freij-Ayoub, R., C. Tan. 2007. A wellbore stability model for hydrate bearing sediments. *Journal of Petroleum Science and Engineering* **57**(1-2): 209-220. doi:10.1016/j.petrol.2005.10.011.

Keller, H. H., Couch E. J. 1973. Temperature Distribution in Circulating Mud Columns. *SPE Journal* **13**(1): 23-30. doi: 10.2118/3605-PA.

Makogon, I. U. 1997. *Hydrates of hydrocarbons*. Tulsa, Oklahoma: PennWell Books.

Moridis, G. J. 2002. Numerical Studies of Gas Production from Methane Hydrates. SPE Gas Technology Symposium, Calgary, Alberta, Canada, 15-16 March. doi:10.2118/87330-PA.

Schofield, T. R., Judzis, A., Yousif, M. 1997. Stabilization of In-situ Hydrates Enhances Drilling Performance and Rig Safety. SPE Annual Technical Conference and Exhibition. San Antonio, Texas, USA, SPE. 4- 7 November. doi:10.2118/38568-MS.

Sloan, J. E. D. 1998. *Clathrane Hydrates of Natural Gases*, New York: Marcel Dekker Inc.

Tsypkin, G. G. 2000. Mathematical Models of Gas Hydrate Dissociation in Porous Media: Gas Hydrate Challenges for the Future. *NY Academy of Sciences* **912**: 428-436. doi:10.1111/j.1749-6632.2000.tb06797.x.

Yousif, M. H., Abass H. H. 1991. Experimental and Theoretical Investigation of Methane-Gas-Hydrate Dissociation in Porous Media. *SPE Reservoir Engineering* **6**(1): 69-76. doi:10.2118/18320-PA.

APPENDIX A

This code calculates:

1. PT distribution in formation during GH decomposition due to pressure drop (Axis-Symmetrical Problem)
2. Rate of decomposed gas

Tagir Khabibullin 2009

Input Parameters:
Formation (rock) Parameters:

```
 μ = 0.0035;
q = 1; (*rate of the gas circulation in drilling mud*)
m = 0.01;
h = 60;
k₁ = 1;
k₂ = 0;
pₑ = 10000;
tₑ = 278;
a₁ = 1; (*thermal conductivity*)
a₂ = 2;
α1 = 1; (*heat capacity*)
α2 = 2;
```

G-H parameres:

```
 σ = 0 ;(*water content of pores*)
β = 1; (*hydrate saturation of a layer*)
ρc = 1;(*volume heat capacity of gas*)
δ = 1; (*throttling coefficient of gas*)
η = 1;(*adiabatic coefficient of gas*)
a = 0.0342; (*K^-1,*empirical constants*)
b = 0.0005; (*K^-2*)
c = 6.4804;
t₀ = 273;
ρ0 = 1; (*density of gas at atmospheric PT*)
p₀ = 100000;
p_G = 90000;
mm = 28; (*molecular mass of the gas*)
l = 10; (*ratio of number of water molecules per one
molecule of gas in a hydrate*)
```
Intermediary parameners:
```
 χ1 = k₁*p_wb/(m*(1-σ)*μ);
χ2 = k₂*pₑ/(m*(1-β)*μ);
λ1 = r/(2*(\[Sqrt](χ1*t)));
```

```
λ2 = r/(2*(\[Sqrt](χ2*t)));
α1 = \[Sqrt](γ/(4*χ1));
α2 = \[Sqrt](γ/(4*χ2));
αI =
 αII =
```

Solution:

```
     ε=mm/(18*l+mm)  ;(*mass fraction of gas in hydrate*)
    A1=2*(Subscript[p, d]²-Subscript[p, g]²)/(Erf[λ1]*p_g);
    A2 =2*(Subscript[p, e]²-Subscript[p, d]²)/(Erf[λ2]*p_e);
    B1 = Subscript[p, g]²*m_1*ρ0C/(4*p_0*αI);
    B2 = Subscript[p, e]²*m_2*ρ0C/(4*p_0*αII);
```

$$p_d = 10^{\left(a*(t_d-t_0)+b*(t_d-t_0)^2+c\right)}; \quad (*\text{dissociation pressure}*)$$

```
C1 =( Subscript[p, d]²-Subscript[p,
g]²)*ρ0C*k_1/(p_g*αI*2*Sqrt[Pi]*Erf[λ1]*μ*χ1);
C2 =( Subscript[p, e]²-Subscript[p,
d]²)*ρ0C*k_2/(p_e*αII*2*Sqrt[Pi]*Erf[λ2]*μ*χ2);

t_d=t_e+A2*δ *Log[Erfc[α2]+(1+η*B2/δ)*(2/Pi)*Integrate[η*Exp[-
η2]/(η+C2*Exp[-η2]),η,α2,Infinity]];  (*dissociation
temperature*)

(*--------Pressure distribution-------------*)
p_1 =\[Sqrt](Subscript[p, d]²+q*μ*p_0*(ExpIntegralEi[-
Subscript[λ, 1]²]-ExpIntagralEi[-Subscript[α,
1]²])/(Pi*k_1*h));
p_2 = \[Sqrt](Subscript[p, e]²+(Subscript[p, d]²-Subscript[p,
e]²)*(ExpIntegralEi[-Subscript[λ, 2]²]/ExpIntagralEi[-
Subscript[α, 2]²]));


t_1=t_d+A1*(ExpIntegralEi[-Subscript[λ,
1]²]+(1+q_1)*ExpIntegralEi[(-Subscript[λ, 1]²-B1*Exp[-
Subscript[λ, 1]²])]-ExpIntagralEi[-Subscript[α, 1]²]-
(1+q_1)*ExpIntagralEi[(-Subscript[α, 1]²-B1*Exp[-Subscript[α,
1]²])])
t_2= t_e+A2*(ExpIntegralEi[-Subscript[λ,
2]²]+(1+q_2)*ExpIntegralEi[(-Subscript[λ, 2]²-B2*Exp[-
Subscript[λ, 2]²])]);

q*μ*p_0*Exp[-Subscript[α, 1]²]/(Pi*h*ρ0)+k_2*(Subscript[p, e]²-
Subscript[p, d]²)*Exp[-Subscript[α, 2]²]/ExpIntegralEi[-
Subscript[α, 2]²]=(β*ε*ρ3*p_0*z/ρ0-(β-
σ)*p_d)*χ1*μ*m*α1{\pard{PPENDIX}
```

APPENDIX B

```
Input_for _simulation_run_1: Equilibrium dissociation of hydrate,
TOUGH-Fx MEMORY ALLOCATION
HYDRATE-EQUILIBRIUM
    2    3    3    0    2      ! NK,NEQ,NPH,M_BinDif,M_add
        015       030 5       ! MNEL,MNCON,No_CEN,FLG_con
    2                         ! MaxNum_SS
    2                         ! MaxNum_Media
ROCKS----1----*----2----*----3----*----4----*----5----*----6----*----7-
---*----8
DIRT1   1    2.6e3        .30  2.96E-13  2.96E-13  2.96E-13        3.0
1000.
     1.e-8              7.0e-1
BOUND   0    2.6e3       0.0e0  0.00E-13  0.00E-13  0.00E-13      1.0e2
1000.

HYDRATE--1----*----2----*----3----*----4----*----5----*----6----*----7-
---*----8
    1                         ! HCom%NCom
'CH4'  6.0d0 1.00d00         ! Name, hydration number, mole fraction in
composite hydrate
    1                         ! Number of coefficients in thermal
conductivity polynomial
  4.5e-1                      ! Coefficients in the thermal conductivity
polynomial
    1                         ! Number of coefficients in the specific
heat polynomial
  2.1e03                      ! Coefficients in the specific heat
polynomial
    1                         ! Number of coefficients in density
polynomial
  9.2e02                      ! Coefficients in the density polynomial
5.0d0  1.0d-2 58.448e0 2.6e3  6.6479d4 1.3d-9 !
T_MaxOff,C_MaxOff,MW_Inhib,D_Inhib,H_InhSol,DifCo_Inh
0                             ! F_EqOption
'EQUILIBRIUM'                 ! Type of dissociation
START----1----*----2----*----3----*----4----*----5----*----6----*----7-
---*----8
----*----1 MOP: 123456789*123456789*1234 ---*----5----*----6----*----7-
---*----8
PARAM----1----*----2----*----3----*----4----*----5----*----6----*----7-
---*----8
    3 080    0021000301000000000400003000   0.00E-5
            8.640E+5    1.0e00    8.64E+6                  9.8060
     1.E-5     1.E00                                       1.0e-8
AqH
            6.000e6                5.0e-1                   7.20
ELEME
A00 1            10.1000E+000.4000E+00          0.5100E-01-.5000E+00-
.5000E+00
```

```
A00 2            10.1000E+000.4000E+00        0.1510E+00-.5000E+00-
.5000E+00
A00 3            10.1000E+000.4000E+00        0.2510E+00-.5000E+00-
.5000E+00
A00 4            10.1000E+000.4000E+00        0.3510E+00-.5000E+00-
.5000E+00
A00 5            10.1000E+000.4000E+00        0.4510E+00-.5000E+00-
.5000E+00
A00 6            10.1000E+000.4000E+00        0.5510E+00-.5000E+00-
.5000E+00
A00 7            10.1000E+000.4000E+00        0.6510E+00-.5000E+00-
.5000E+00
A00 8            10.1000E+000.4000E+00        0.7510E+00-.5000E+00-
.5000E+00
A00 9            10.1000E+000.4000E+00        0.8510E+00-.5000E+00-
.5000E+00
A0010            10.1000E+000.4000E+00        0.9510E+00-.5000E+00-
.5000E+00
ina
A00 0            10.1000E-020.4000E-02        0.5000E-03-.5000E+00-
.5000E+00


CONNE
A00 0A00 1                 10.5000E-030.5000E-010.1000E+01
A00 1A00 2                 10.5000E-010.5000E-010.1000E+01
A00 2A00 3                 10.5000E-010.5000E-010.1000E+01
A00 3A00 4                 10.5000E-010.5000E-010.1000E+01
A00 4A00 5                 10.5000E-010.5000E-010.1000E+01
A00 5A00 6                 10.5000E-010.5000E-010.1000E+01
A00 6A00 7                 10.5000E-010.5000E-010.1000E+01
A00 7A00 8                 10.5000E-010.5000E-010.1000E+01
A00 8A00 9                 10.5000E-010.5000E-010.1000E+01
A00 9A0010                 10.5000E-010.5000E-010.1000E+01
A0010A0011                 10.5000E-010.5000E-030.1000E+01


RPCAP----1----*----2----*----3----*----4----*----5----*----6----*----7-
---*----8
    6         .150        .05        .001        3.
    8        0.140       1.84        10.        11.
COFT -----1----*----2----*----3----*----4----*----5----*----6----*----
7----*----8
A00 0A00 1


GENER


INCON----1----*----2----*----3----*----4----*----5----*----6----*----7-
---*----8
A00 0          0.30000000E+00  Aqu
          2.700e6              00.0e0                  1.00
```

```
ENDCY----1----*----2----*----3----*----4----*----5----*----6----*----7-
---*----8

MESHMAKER1----*----2----*----3----*----4----*----5----*----6----*----7-
---*----8
XYZ
       00.
NX      1   1.0e-3
NX     10   1.0e-1
NX      1   1.0e-3
NY      1      1.0
NZ      1      1.0


ENDFI
```

VITA

Name: Tagir R. Khabibullin

Address: Harold Vance Department of Petroleum Engineering
                     Texas A&M University
                     3116 TAMU 602 Richardson Building
                     College Station, TX 77843-3116

Email Address: tagir_khabibullin@yahoo.com

Education: B.S., Petroleum Engineering, Ufa State Petroleum Technological

                     University, Ufa, 2008

                     M.S., Petroleum Engineering, Texas A&M University, 2010